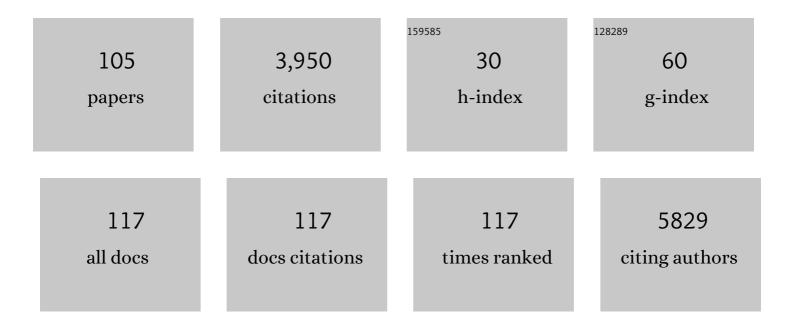
## **Roland Marschall**

List of Publications by Year in descending order

Source: https://exaly.com/author-pdf/2901210/publications.pdf Version: 2024-02-01



#	Article	IF	CITATIONS
1	Semiconductor Composites: Strategies for Enhancing Charge Carrier Separation to Improve Photocatalytic Activity. Advanced Functional Materials, 2014, 24, 2421-2440.	14.9	1,293
2	Non-metal doping of transition metal oxides for visible-light photocatalysis. Catalysis Today, 2014, 225, 111-135.	4.4	311
3	Nâ€Doped CsTaWO <sub>6</sub> as a New Photocatalyst for Hydrogen Production from Water Splitting Under Solar Irradiation. Advanced Functional Materials, 2011, 21, 126-132.	14.9	135
4	Ordered Functionalized Silica Materials with High Proton Conductivity. Chemistry of Materials, 2007, 19, 6401-6407.	6.7	90
5	Proton conductivity of sulfonic acid functionalised mesoporous materials. Microporous and Mesoporous Materials, 2007, 99, 190-196.	4.4	84
6	Preparation of porous composite ion-exchange membranes for desalination application. Journal of Materials Chemistry, 2011, 21, 7401.	6.7	83
7	Synthesis of composite ion-exchange membranes and their electrochemical properties for desalination applications. Journal of Materials Chemistry, 2010, 20, 4669.	6.7	68
8	Preparation of new sulfur-doped and sulfur/nitrogen co-doped CsTaWO6 photocatalysts for hydrogen production from water under visible light. Journal of Materials Chemistry, 2011, 21, 8871.	6.7	66
9	Enhanced photocatalytic hydrogen generation from barium tantalate composites. Photochemical and Photobiological Sciences, 2013, 12, 671-677.	2.9	57
10	Nanoparticles of Mesoporous SO <sub>3</sub> Hâ€Functionalized Siâ€MCMâ€41 with Superior Proton Conductivity. Small, 2009, 5, 854-859.	10.0	54
11	New proton conducting hybrid membranes for HT-PEMFC systems based on polysiloxanes and SO3H-functionalized mesoporous Si-MCM-41 particles. Journal of Membrane Science, 2008, 316, 164-175.	8.2	53
12	Heterogeneous Photoredox Catalysis: Reactions, Materials, and Reaction Engineering. European Journal of Organic Chemistry, 2017, 2017, 2085-2094.	2.4	51
13	Electrochemical CO <sub>2</sub> Reduction: Tailoring Catalyst Layers in Gas Diffusion Electrodes. Advanced Sustainable Systems, 2021, 5, 2000088.	5.3	50
14	Improved overall water splitting with barium tantalate mixed oxide composites. Chemical Science, 2014, 5, 3746-3752.	7.4	49
15	Stabilization of Monodisperse, Phase-Pure MgFe <sub>2</sub> O <sub>4</sub> Nanoparticles in Aqueous and Nonaqueous Media and Their Photocatalytic Behavior. Journal of Physical Chemistry C, 2017, 121, 27126-27138.	3.1	45
16	Layered Perovskite Nanofibers via Electrospinning for Overall Water Splitting. Small, 2015, 11, 2051-2057.	10.0	44
17	Proton conductivity of imidazole functionalized ordered mesoporous silica: Influence of type of anchorage, chain length and humidity. Microporous and Mesoporous Materials, 2009, 123, 21-29.	4.4	43
18	Correlating Changes in Electron Lifetime and Mobility on Photocatalytic Activity at Network-Modified TiO <sub>2</sub> Aerogels, Journal of Physical Chemistry C. 2015, 119, 17529-17538.	3.1	42

#	Article	IF	CITATIONS
19	Control of Phase Coexistence in Calcium Tantalate Composite Photocatalysts for Highly Efficient Hydrogen Production. Chemistry of Materials, 2013, 25, 4739-4745.	6.7	41
20	Pitfalls in Heterogeneous Thermal, Electro―and Photocatalysis. ChemCatChem, 2019, 11, 2563-2574.	3.7	41
21	50 Years of Materials Research for Photocatalytic Water Splitting. European Journal of Inorganic Chemistry, 2021, 2021, 2435-2441.	2.0	41
22	Development of polyoxadiazole nanocomposites for high temperature polymer electrolyte membrane fuel cells. Journal of Membrane Science, 2008, 322, 406-415.	8.2	38
23	Hollow α-Fe <sub>2</sub> O <sub>3</sub> nanofibres for solar water oxidation: improving the photoelectrochemical performance by formation of α-Fe <sub>2</sub> O <sub>3</sub> /ITO-composite photoanodes. Journal of Materials Chemistry A, 2016, 4, 18444-18456.	10.3	37
24	Deconstructing collagen piezoelectricity using alanine-hydroxyproline-glycine building blocks. Nanoscale, 2018, 10, 9653-9663.	5.6	36
25	Sol–gel synthesis of defect-pyrochlore structured CsTaWO6 and the tribochemical influences on photocatalytic activity. RSC Advances, 2013, 3, 18908.	3.6	34
26	Mesoporous Semiconductors: A New Model To Assess Accessible Surface Area and Increased Photocatalytic Activity?. ACS Applied Energy Materials, 2018, 1, 5787-5799.	5.1	34
27	Flexible, Mechanically Stable, Porous Self‣tanding Microfiber Network Membranes of Covalent Organic Frameworks: Preparation Method and Characterization. Advanced Functional Materials, 2021, 31, 2106507.	14.9	34
28	Tetragonal tungsten bronze-type nanorod photocatalysts with tunnel structures: Ta substitution for Nb and overall water splitting. Journal of Materials Chemistry A, 2014, 2, 8815-8822.	10.3	33
29	Exploring wet chemistry approaches to ZnFe <sub>2</sub> O <sub>4</sub> spinel ferrite nanoparticles with different inversion degrees: a comparative study. Inorganic Chemistry Frontiers, 2019, 6, 1527-1534.	6.0	32
30	Pore Structure Controlling the Activity of Mesoporous Crystalline CsTaWO <sub>6</sub> for Photocatalytic Hydrogen Generation. Advanced Energy Materials, 2016, 6, 1600208.	19.5	31
31	Characterization of MFe <sub>2</sub> O <sub>4</sub> (M = Mg, Zn) Thin Films Prepared by Pulsed Laser Deposition for Photoelectrochemical Applications. Journal of Physical Chemistry C, 2019, 123, 18240-18247.	3.1	31
32	Insight into Proton Conduction of Immobilised Imidazole Systems Via Simulations and Impedance Spectroscopy. Fuel Cells, 2008, 8, 244-253.	2.4	30
33	Photocatalysis: Semiconductor Composites: Strategies for Enhancing Charge Carrier Separation to Improve Photocatalytic Activity (Adv. Funct. Mater. 17/2014). Advanced Functional Materials, 2014, 24, 2420-2420.	14.9	30
34	Electrospun CuO Nanofibers: Stable Nanostructures for Solar Water Splitting. ChemPhotoChem, 2017, 1, 326-340.	3.0	30
35	Detailed Simulation and Characterization of Highly Proton Conducting Sulfonic Acid Functionalized Mesoporous Materials under Dry and Humidified Conditions. Journal of Physical Chemistry C, 2009, 113, 19218-19227.	3.1	28
36	Proton transport in functionalised additives for PEM fuel cells: contributions from atomistic simulations. Chemical Society Reviews, 2012, 41, 5143.	38.1	27

#	Article	IF	CITATIONS
37	Composite proton-conducting polymer membranes for clean hydrogen production with solar light in a simple photoelectrochemical compartment cell. International Journal of Hydrogen Energy, 2012, 37, 4012-4017.	7.1	27
38	Layered Dion-Jacobson type niobium oxides for photocatalytic hydrogen production prepared via molten salt synthesis. Catalysis Today, 2017, 287, 65-69.	4.4	27
39	Tailoring the Size, Inversion Parameter, and Absorption of Phase-Pure Magnetic MgFe <sub>2</sub> O <sub>4</sub> Nanoparticles for Photocatalytic Degradations. ACS Applied Nano Materials, 2020, 3, 11587-11599.	5.0	27
40	Understanding the Influence of Lattice Composition on the Photocatalytic Activity of Defectâ€Pyrochloreâ€Structured Semiconductor Mixed Oxides. Advanced Functional Materials, 2015, 25, 905-912.	14.9	26
41	Passivation layers for nanostructured photoanodes: ultra-thin oxides on InGaN nanowires. Journal of Materials Chemistry A, 2018, 6, 565-573.	10.3	26
42	Magnesium Ferrite (MgFe <sub>2</sub> O <sub>4</sub> ) Nanoparticles for Photocatalytic Antibiotics Degradation. Zeitschrift Fur Physikalische Chemie, 2020, 234, 645-654.	2.8	26
43	Improved charge carrier separation in barium tantalate composites investigated by laser flash photolysis. Physical Chemistry Chemical Physics, 2016, 18, 10719-10726.	2.8	25
44	A crystalline and 3D periodically ordered mesoporous quaternary semiconductor for photocatalytic hydrogen generation. Nanoscale, 2018, 10, 3225-3234.	5.6	25
45	Layered cesium copper titanate for photocatalytic hydrogen production. Applied Catalysis B: Environmental, 2018, 227, 349-355.	20.2	23
46	Photocatalytic activity of multiphase TiO2(B)/anatase nanoparticle heterojunctions prepared from ionic liquids. Journal of Photochemistry and Photobiology A: Chemistry, 2018, 366, 34-40.	3.9	22
47	Mesoporous ZnFe 2 O 4 Photoanodes with Templateâ€Tailored Mesopores and Temperatureâ€Đependent Photocurrents. ChemPhysChem, 2018, 19, 2313-2320.	2.1	22
48	Detection of Homogeneous Distribution of Functional Groups in Mesoporous Silica by Small Angle Neutron Scattering and in Situ Adsorption of Nitrogen or Water. Langmuir, 2011, 27, 5516-5522.	3.5	21
49	Single crystal CsTaWO 6 nanoparticles for photocatalytic hydrogen production. Nano Energy, 2017, 31, 551-559.	16.0	21
50	Magnetic NiFe <sub>2</sub> O <sub>4</sub> Nanoparticles Prepared via Nonâ€Aqueous Microwaveâ€Assisted Synthesis for Application in Electrocatalytic Water Oxidation. Chemistry - A European Journal, 2021, 27, 16990-17001.	3.3	21
51	Tailoring the diameter of electrospun layered perovskite nanofibers for photocatalytic water splitting. Journal of Materials Chemistry A, 2018, 6, 1971-1978.	10.3	17
52	Sol–gel synthesis of mesoporous CaFe <sub>2</sub> O <sub>4</sub> photocathodes with hierarchical pore morphology. Sustainable Energy and Fuels, 2019, 3, 1150-1153.	4.9	16
53	Photoinduced Defect and Surface Chemistry of Niobium Tellurium Oxides ANbTeO <sub>6</sub> (A = K,) Tj ETQ	q1 1.0.784 4.0	1314 rgBT /○ 16
54	Photocatalytic Nitrogen Reduction: Challenging Materials with Reaction Engineering. ChemPhotoChem, 2021, 5, 792-807.	3.0	16

#	Article	IF	CITATIONS
55	Thermal Evolution of ZnS Nanostructures: Effect of Oxidation Phenomena on Structural Features and Photocatalytical Performances. Inorganic Chemistry, 2018, 57, 13104-13114.	4.0	15
56	Sulfonation of porous materials and their proton conductivity. Microporous and Mesoporous Materials, 2021, 312, 110745.	4.4	15
57	Mesoporous NiFe <sub>2</sub> O <sub>4</sub> with Tunable Pore Morphology for Electrocatalytic Water Oxidation. ChemElectroChem, 2021, 8, 227-239.	3.4	15
58	An investigation of the optical properties and water splitting potential of the coloured metallic perovskites Sr1â^'Ba MoO3. Journal of Solid State Chemistry, 2016, 234, 87-92.	2.9	13
59	Sulfonated Mesoporous Silica as Proton Exchanging Layer in Solidâ€ <del>S</del> tate Organic Transistor. Advanced Electronic Materials, 2017, 3, 1700316.	5.1	13
60	Proton Conduction in Sulfonated Organic–Inorganic Hybrid Monoliths with Hierarchical Pore Structure. ACS Applied Materials & Interfaces, 2016, 8, 25476-25488.	8.0	12
61	Aqueous Sol–Gel Route toward Selected Quaternary Metal Oxides with Single and Double Perovskite-Type Structure Containing Tellurium. Crystal Growth and Design, 2016, 16, 2535-2541.	3.0	12
62	Selfâ€Assembled Fluorescent Block Copolymer Micelles with Responsive Emission. Angewandte Chemie - International Edition, 2022, 61, .	13.8	12
63	Fe <sub>x</sub> Ni <sub>9â^'x</sub> S <sub>8</sub> ( <i>x</i> = 3–6) as potential photocatalysts for solar-driven hydrogen production?. Faraday Discussions, 2019, 215, 216-226.	3.2	11
64	Heterojunctions in Composite Photocatalysts. Topics in Current Chemistry, 2015, 371, 143-172.	4.0	10
65	Magnetic properties and structural analysis on spinel MnFe <sub>2</sub> O <sub>4</sub> nanoparticles prepared <i>via</i> nonâ€aqueous microwave synthesis. Zeitschrift Fur Anorganische Und Allgemeine Chemie, 2021, 647, 2061-2072.	1.2	10
66	Active Sites for Light Driven Proton Reduction in Y2Ti2O7 and CsTaWO6 Pyrochlore Catalysts Detected by In Situ EPR. Topics in Catalysis, 2015, 58, 769-775.	2.8	9
67	A Novel Synthesis Yielding Macroporous CaFe <sub>2</sub> O <sub>4</sub> Sponges for Solar Energy Conversion. Solar Rrl, 2020, 4, 1900570.	5.8	9
68	Fast Microwave Synthesis of Phase-Pure Ni <sub>2</sub> FeS <sub>4</sub> Thiospinel Nanosheets for Application in Electrochemical CO <sub>2</sub> Reduction. ACS Applied Energy Materials, 2021, 4, 8702-8708.	5.1	9
69	Proton conductivity of ordered mesoporous materials containing aluminium. Journal of Power Sources, 2010, 195, 7781-7786.	7.8	8
70	New insight into calcium tantalate nanocomposite photocatalysts for overall water splitting and reforming of alcohols and biomass derivatives. APL Materials, 2015, 3, 104412.	5.1	8
71	A Novel and Versatile Grafting Procedure: Toward the Highest Possible Sulfonation Degree of Mesoporous Silica. Advanced Sustainable Systems, 2018, 2, 1700170.	5.3	8
72	Ordered Mesoporous LiFe 5 O 8 Thinâ€Film Photoanodes for Water Splitting. ChemPhotoChem, 2018, 2, 1022-1026.	3.0	8

#	Article	IF	CITATIONS
73	A highly porous and conductive composite gate electrode for OTFT sensors. RSC Advances, 2019, 9, 7278-7284.	3.6	8
74	Electrospun CuO Nanofibre Assemblies for H <sub>2</sub> S Sensing. Zeitschrift Fur Physikalische Chemie, 2018, 233, 105-116.	2.8	7
75	The Influence of Tin(II) Incorporation on Visible Light Absorption and Photocatalytic Activity in Defectâ€Pyrochlores. Chemistry - A European Journal, 2018, 24, 18535-18543.	3.3	7
76	Layered Perovskite Nanofiber Heterojunctions with Tailored Diameter to Enhance Photocatalytic Water Splitting Performance. ACS Applied Energy Materials, 2018, 1, 2520-2525.	5.1	7
77	Synthesis of hydrated KTaWO <sub>6</sub> nanoparticles and Sn( <scp>ii</scp> ) incorporation for visible light absorption. Nanoscale, 2018, 10, 9691-9697.	5.6	7
78	Independent Tailoring of Macropore and Mesopore Space in TiO <sub>2</sub> Monoliths. Inorganic Chemistry, 2019, 58, 2599-2609.	4.0	7
79	Immobilization of a copper complex based on the tripodal ligand (2â€aminoethyl)bis(2â€pyridylmethyl)amine (unsâ€penp). Zeitschrift Fur Anorganische Und Allgemeine Chemie, 2021, 647, 560-571.	1.2	7
80	Highly mesoporous CsTaWO <sub>6</sub> via hard-templating for photocatalytic hydrogen production. RSC Advances, 2016, 6, 79037-79042.	3.6	6
81	Perovskiteâ€Type Oxynitride Nanofibers Performing Photocatalytic Oxygen and Hydrogen Generation. Advanced Materials Interfaces, 2021, 8, 2100813.	3.7	6
82	PrÃ <b>p</b> aration und Evaluation neuer Hybridâ€Protonenleiter – Teil II: Anorganische Nanoteilchen als Modifikator in Nafion®â€Hybridmembranen. Chemie-Ingenieur-Technik, 2007, 79, 2035-2041.	0.8	5
83	Stabilization of nanosized MgFe2O4 nanoparticles in phenylene-bridged KIT-6-type ordered mesoporous organosilica (PMO). Microporous and Mesoporous Materials, 2020, 293, 109783.	4.4	5
84	Spin States of 1D Iron(II) Coordination Polymers with Redox Active TTF(py) <sub>2</sub> as Bridging Ligand. Zeitschrift Fur Anorganische Und Allgemeine Chemie, 2021, 647, 295-305.	1.2	5
85	The Elemental Multifariousness of the Defectâ€Pyrochlore Crystal Structure and Application in Photocatalytic Hydrogen Generation. Energy Technology, 0, , 2100302.	3.8	5
86	[NiFe]-(Oxy)Sulfides Derived from NiFe2O4 for the Alkaline Hydrogen Evolution Reaction. Energies, 2022, 15, 543.	3.1	5
87	Tuning the photocatalytic activity of layered perovskite niobates by controlled ion exchange and hydration. Catalysis Science and Technology, 2022, 12, 1450-1457.	4.1	5
88	Experimental correlation of Mn <sup>3+</sup> cation defects and electrocatalytic activity of α-MnO <sub>2</sub> – an X-ray photoelectron spectroscopy study. Journal of Materials Chemistry A, 2022, 10, 15811-15838.	10.3	5
89	Rational fabrication of a graphitic-C <sub>3</sub> N <sub>4</sub> /Sr <sub>2</sub> KNb <sub>5</sub> O <sub>15</sub> nanorod composite with enhanced visible-light photoactivity for degradation of methylene blue and hydrogen production. RSC Advances. 2017. 7, 42774-42782.	3.6	4
90	Functionalized mesoporous materials used as proton conductive additives for high temperature PEM fuel cell membranes. Studies in Surface Science and Catalysis, 2007, 170, 1540-1545.	1.5	3

#	Article	IF	CITATIONS
91	Protonâ€Conducting Composite Membranes for Future Perspective Applications in Fuel Cells, Desalination Facilities and Photocatalysis. Chemie-Ingenieur-Technik, 2011, 83, 2177-2187.	0.8	3
92	Fast low temperature synthesis of layered perovskite heterojunctions for overall water splitting. JPhys Energy, 2021, 3, 014002.	5.3	3
93	Nâ€Ðoped CsTaWO <sub>6</sub> as a New Photocatalyst for Hydrogen Production from Water Splitting Under Solar Irradiation. Advanced Functional Materials, 2011, 21, 125-125.	14.9	2
94	German Catalysis on an International Scale in Weimar. ChemCatChem, 2014, 6, 1523-1525.	3.7	2
95	Weimar 2015: Catalysing Tomorrow's Solutions. ChemCatChem, 2015, 7, 1794-1796.	3.7	2
96	Corrigendum to Layered Dion-Jacobson type niobium oxides for photocatalytic hydrogen production prepared via molten salt synthesis. Catalysis Today, 2020, 353, 213.	4.4	2
97	Terrestrial solar radiation driven photodecomposition of ciprofloxacin in clinical wastewater applying mesostructured iron(III) oxide. Environmental Science and Pollution Research, 2021, 28, 6222-6231.	5.3	2
98	Organosilica Nanoparticles with Ordered Trimodal Porosity and Selectively Functionalized Mesopores. Chemie-Ingenieur-Technik, 2022, 94, 101-110.	0.8	1
99	Acceleration of electrocatalytic CO <sub>2</sub> reduction by adding proton-coupled electron transfer inducing compounds. Journal of Photonics for Energy, 0, , 012001.	1.3	0
100	Sensors: Sulfonated Mesoporous Silica as Proton Exchanging Layer in Solidâ€ <b>s</b> tate Organic Transistor (Adv. Electron. Mater. 12/2017). Advanced Electronic Materials, 2017, 3, 1770055.	5.1	0
101	TEXTURAL INVESTIGATIONS OF HIGHLY PROTON CONDUCTIVE FUNCTIONALIZED MESOPOROUS SIO2. , 2008,		0
102	Electrospinning to Prepare Nanostructured Photocatalysts and Photoelectrodes. ECS Meeting Abstracts, 2018, MA2018-01, 1905-1905.	0.0	0
103	Selfâ€Assembled Fluorescent Block Copolymer Micelles with Responsive Emission. Angewandte Chemie, 0, , .	2.0	0
104	Frontispiz: Selbstassemblierte fluoreszierende Blockcopolymerâ€Mizellen mit responsiver Emission. Angewandte Chemie, 2022, 134, .	2.0	0
105	Frontispiece: Selfâ€Assembled Fluorescent Block Copolymer Micelles with Responsive Emission. Angewandte Chemie - International Edition, 2022, 61, .	13.8	0